Publication II

Laura Koponen, Lasse Tunturivuori, Martti J. Puska, and Risto M. Nieminen.
2007. Photoabsorption spectra of boron nitride fullerenelike structures. The
Journal of Chemical Physics, volume 126, number 21, 214306, 4 pages.

Photoabsorption spectra of boron nitride fullerenelike structures

Laura Koponen,[a] Lasse Tunturivuori, Martti J. Puska, and Risto M. Nieminen
Laboratory of Physics, Helsinki University of Technology, P.O. Box 1100,
FIN-02015 HUT ESPOO, Finland

Optical absorption spectra have been calculated for a series of boron nitride fullerenelike cage structures B_nN_n of sizes $n=12-36$. The method used is a real-time, real-space implementation of the time-dependent density-functional theory, involving the full time propagation of the time-dependent Kohn-Sham equations. The spectra are found to be a possible tool for distinguishing between different boron nitride fullerene species and isomers. The trends and differences in the spectra are found to be related to the general geometry of the molecules. Comparison between local-density and generalized-gradient approximations for electron exchange-correlation functionals shows that both of them produce essentially the same spectral characteristics. © *2007 American Institute of Physics.*
[DOI: 10.1063/1.2741524]

I. INTRODUCTION

Like carbon, boron nitride (BN) is able to form nanosized structures, for example, fullerenelike cages, onions, and tubes. The fabrication of BN nanotubes[1] and nested cages[2] was reported in the mid-1990s, soon after the discovery of carbon-based fullerenes and related carbon nanostructures. BN fullerenes were synthesized for the first time in 1998 by Stéphan *et al.*[3] These isoelectronic analogs of carbon structures are of interest to both theorists and experimentalists in materials science because of their potential applications in future nano- and optoelectronic devices and also as lubricants. The superiority of BN based structures over the carbon ones would result from their better thermal and chemical stabilities. In this work, the objective is the optical properties of BN fullerenes calculated from first principles. Especially, we want to study their optical absorption spectra which can be used in identifying their structures.

The time-dependent density-functional theory (TDDFT) in its linear-response form is already a standard chemist's tool for calculating optical spectra of small atom clusters and molecules. In contrast to the (time-independent) DFT, the TDDFT can properly treat the excitations of electronic systems (for a review see, for instance, Refs. 4–6). The implementations of the TDDFT are divided into linear-response methods and methods propagating the time-dependent Kohn-Sham equations in real time. Due to the unfavorable scaling of the linear-response methods as the electron number N increases, they become ineffective for structures that consist of several dozens of atoms. Instead, the propagation of the Kohn-Sham equations becomes advantageous despite its large prefactor since it scales linearly with N. This method has been shown to reproduce the main measured low-energy excitations correctly with an accuracy of few tenths of eV for several kinds of systems as long as the time step is small enough and the total propagation time is adequate. It has

been used, for example, for calculating the optical absorption spectra of different B_{20} (Ref. 7) and C_{20} (Ref. 8) isomers.

According to our knowledge, the results presented in this paper are the first TDDFT calculations for BN nanostructures. We are extending the knowledge on the yet almost unexplored optical properties of BN by means of a sophisticated and efficient method. An important aspect of our work is that the structural and spectral properties are calculated on the same footing for a representative set of different BN fullerene structures. This enables the highlighting of differences and trends.

II. STRUCTURES

The basic structural properties of the molecules studied in this work are given in Table I. The molecules are chosen such that they would form a series of energetically favorable structures of BN fullerenes. The following findings from the literature on both experimental results and structure calculations with chemical accuracy have been considered as guidelines for the present work.

It has been found computationally that fullerenelike cage structures B_nN_n are energetically more favorable than ring structures for $n>10$.[9] Unlike carbon fullerenes, BN fullerenes consist purely of rings with even number of atoms. This is caused by the high-energy cost of placing two B or two N atoms next to each other. In computational studies for the fullerene structures most attention has been paid to those with high symmetry. The "magic" octahedronlike structures of $B_{12}N_{12}$, $B_{16}N_{16}$, $B_{28}N_{28}$, and $B_{36}N_{36}$ are found to be especially stable.[10–13] They consist purely of four- and six-membered rings. In contrast, for $B_{24}N_{24}$, the isomers with the lower S_8 and S_4 symmetries are computationally found more stable than the most symmetric isomer with the O symmetry.[14,15] This is due to the high number of energetically less favorable octahedral rings in the O-symmetric structure. However, the differences in total energy are small, of the order of 0.1 eV/at. or less. The same kind of problem is observed in calculations for $B_{32}N_{32}$, the most stable struc-

---

a)Electronic mail: lak@fyslab.hut.fi

126, 214306-1

TABLE I. Molecules studies. Symm. denotes the symmetry point group of the molecule. The numbers of tetragons, hexagons, and octagons that the molecule consists are listed in the Polygons column. Polar. indicates the number of different polarization direction needed when calculating the average spectrum. Schematic pictures of the structures are included in Figs. 1–3.

Species	Symm.	Polygons	Polar.
$B_{12}N_{12}$	T_h	$6F_4+8F_6$	1
$B_{16}N_{16}$	T_d	$6F_4+12F_6$	1
$B_{24}N_{24}$	O	$12F_4+8F_6+6F_8$	1
$B_{24}N_{24}$	S_8	$8F_4+16F_6+2F_8$	2
$B_{24}N_{24}$	S_4	$6F_4+20F_6$	3
$B_{28}N_{28}$	T	$6F_4+24F_6$	1
$B_{36}N_{36}$	T_d	$6F_4+32F_6$	1

ture of which is a totally asymmetric isomer.[16,17] We propose that the determination of the ground-state isomer of $B_{24}N_{24}$ might be found by comparison between the calculated and measured optical spectra rather than between the total energies of different isomers. The IR and Raman spectra calculated in Refs. 15 and 18 can be used in the same manner, enabling complementary comparisons.

On the experimental side the most exhaustive work has been carried out by Oku *et al.*[11–13,19] They have synthesized B_nN_n cages of sizes $n=12–60$ by the arc-melting method and detected them by laser-desorption time-of-flight mass spectroscopy and high-resolution electron microscopy. The profusion of $B_{24}N_{24}$ was remarkable, and also other theoretically stable predicted species were detected abundantly. A novel experimental method on the basis of NMR spectroscopy for revealing the geometrical structures of BN fullerenes is proposed in a preliminary theoretical study.[20]

III. METHOD

The initial structures of the studied BN fullerenes were constructed based on the data in Table I and the literature presented in Sec. II. Then a geometry optimization using the SIESTA program[21] was performed for fine tuning the geometries of the molecules.

The main work was carried out by the OCTOPUS program, a TDDFT real-time real-space code.[22] The full time evolution of the time-dependent Kohn-Sham equations was calculated in OCTOPUS to obtain the dipole strength function, that is to say, the optical absorption spectrum.

Let us briefly summarize the essentials of the TDDFT method used in this work (for further details see, for example, Ref. 23). The system is excited from its initial ground state by applying an instantaneous electric field causing the potential $v(\mathbf{r},t)=-k_0\gamma\delta(t)$, where $\gamma=x,y,z$ denotes the polarization direction and k_0 is the amplitude of the perturbation. This corresponds to multiplying the ground-state wave functions with an exponential $e^{ik_0\gamma}$. Then the system is allowed to propagate over a finite period of time. The dynamical polarizability is

$$\alpha_\gamma(\omega) = -\frac{1}{k_0}\int d^3r\,\gamma\,\delta n(\mathbf{r},\omega), \tag{1}$$

where $\delta n(\mathbf{r},\omega)$ is the time Fourier transform of the deviation of electron density from the ground-state density of the system. The dipole strength function is obtained by averaging over the three spatial coordinates,

$$S(\omega) = \frac{4\pi\omega}{c}\frac{1}{3}\,\text{Im}\left(\sum_\gamma \alpha_\gamma(\omega)\right). \tag{2}$$

Above, c is the speed of light.

Calculations were carried out using two different exchange-correlation potentials: the local-density approximation (LDA) (Ref. 24) and the more advanced Perdew-Burke-Ernzerhof (PBE) generalized-gradient approximation (GGA).[25] Calculations using even more sophisticated methods such as hybrid GGA's, giving the correct asymptotic potential behavior, were not possible due to the limited choice of exchange-correlation functionals implemented in the
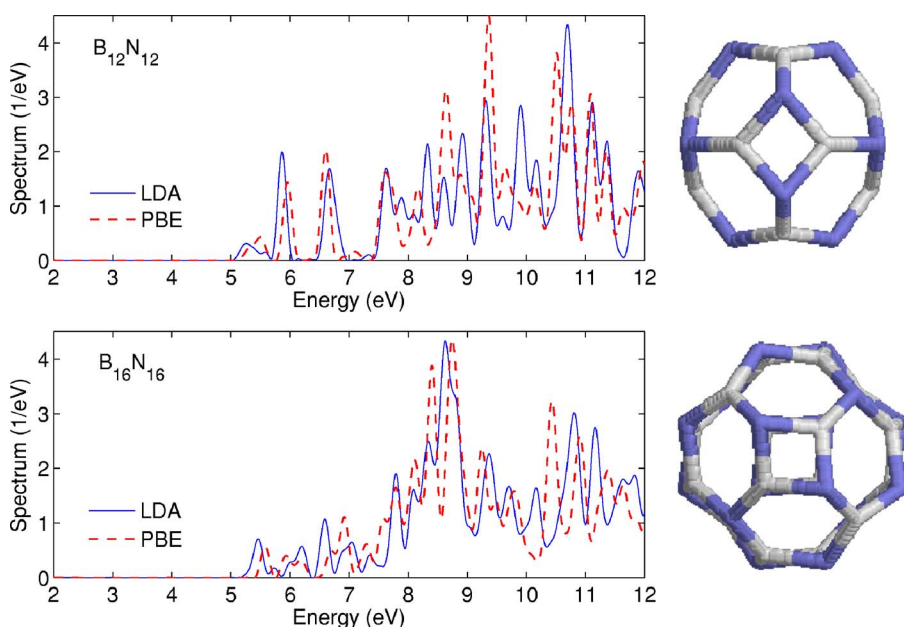

FIG. 1. (Color online) Photoabsorption spectra of $B_{12}N_{12}$ and $B_{16}N_{16}$. The insets on the right-hand side show the optimized structures of the molecules.
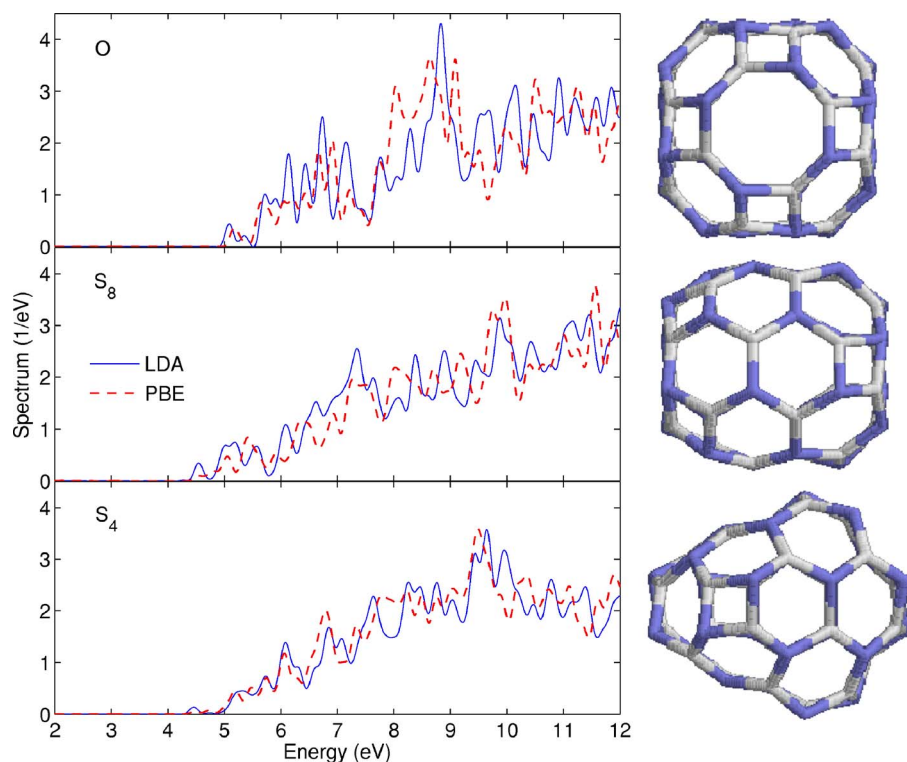
FIG. 2. (Color online) Photoabsorption spectra of three different isomers of $B_{24}N_{24}$: O, S_8, and S_4 isomers. The insets on the right-hand side show the optimized structures of the molecules.

current stable version of the OCTOPUS program. The norm-conserving Troullier-Martins pseudopotentials[26] were used throughout the calculations. The double ζ with polarization basis set was used in the SIESTA calculations. The numerical parameters in the OCTOPUS calculations were the following: time step of $0.0025\hbar/eV$, total propagation time of $37.5\hbar/eV$, spacing of real-space mesh points of 0.3 Å, and radius of wave function domain around each nucleus of $6-8$ Å. The calculations correspond to zero temperature.

IV. RESULTS

The structure optimization resulted in bond lengths varying over the range of $1.41-1.49$ Å ($1.43-1.50$ Å) when employing the LDA (PBE) scheme. The structures, their bond lengths, and total energies were in good accordance with the literature cited in Sec. II. Further details of the structure optimization results are not given here, as the calculation of optical spectra is not sensitive to small variations in the structure.

The spectra of all studied molecules can be divided into three energy regions. First, no excitations occur at energies below the highest occupied molecular orbital–lowest unoccupied molecular orbital gap. In the interesting region of about $5-10$ eV several peaks appear, the details depending on the structure. Above that a broad feature extends up to several tens of eV's. Most of the strength of the spectra is found here, but this high-energy region has little interest since it is more cumbersome to access experimentally. In
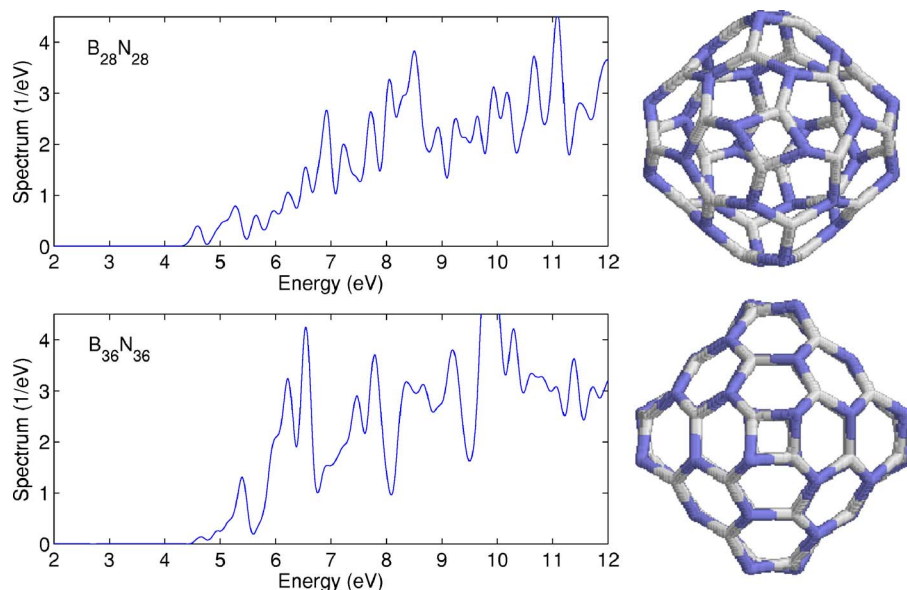

FIG. 3. (Color online) Photoabsorption spectra of $B_{28}N_{28}$ and $B_{36}N_{36}$. The insets on the right-hand side show the optimized structures of the molecules. LDA approximation has been used.

addition, the method we used is insufficient to describe the behavior of the electrons in the high-energy region because it is dominated by ionization processes.

The results were both qualitatively and quantitatively quite similar for LDA and PBE. The number and grouping of the excitation peaks agree well and the intensities of the peaks follow similar trends. This is in accordance with other studies, for example, Ref. 27. Compared to the static DFT, where GGA clearly beats LDA in predicting structural properties, the situation is different in TDDFT. The only systematic difference observed in this study is the slightly larger energy gaps obtained by PBE.

The spectra of the smallest studied molecules, $B_{12}N_{12}$ and $B_{16}N_{16}$, are shown in Fig. 1. $B_{12}N_{12}$ has sharp excitations at about 5.9 and 6.6 eV and a minor one around 5.2–5.5 eV. In the range of 7.5–10 eV several additional sharp peaks are observed. For $B_{16}N_{16}$ the major excitations take place around 8.5 eV, with several minor peaks in the range of 5.3–8 eV. The excitation gap is 5.0 eV (5.1 eV) for $B_{12}N_{12}$ and 5.2 eV (5.4 eV) for $B_{16}N_{16}$, according to the LDA (PBE) calculations. The excitation gaps are in good accordance with, for example, the ones calculated in Ref. 10.

For the larger molecules, the interesting 5–10 eV part of the spectra becomes fuzzier as it is observed in Figs. 2 and 3. However, some trends can be observed, for example, between the different isomers of $B_{24}N_{24}$. The symmetric O isomer exhibits sharp peaks around 7 and 9 eV, whereas the spectra of S_8 and S_4 isomers are flatter. This is due to the larger variety of different bond lengths and orientations in asymmetric molecules. The clearest peaks are identified around 9.5 eV for the S_8 isomer and around 10 eV for the S_4 isomer. The symmetric O isomer has an excitation gap of 5.0 eV, whereas the S_8 and S_4 isomers show clearly smaller gaps of about 4.3 eV. This difference is also explained by geometric arguments. The asymmetric isomers have a longer spatial dimension in one direction, involving longer π orbital chains. This implies a stronger delocalization of the valence electrons in that direction and thus a decrease in the gap.

According to Fig. 3, $B_{28}N_{28}$ shows a series of close peaks starting from 4.5 eV. The spectrum of $B_{36}N_{36}$ in Fig. 3 is more distinctive with larger features: the lowest peaks are observed at 5.4, 6.0–6.7, and 7.4–7.9. The excitation gaps are 4.4 eV (4.9 eV) for $B_{28}N_{28}$ and 4.5 eV (4.7 eV) for $B_{36}N_{36}$ using the LDA (PBE) scheme. Our spectrum of $B_{36}N_{36}$ based on the TDDFT is much more complex and even qualitatively different from the one calculated on the DFT level in Ref. 16. A spectrum predicted correctly to the extent of the details is of vital importance for the identification of the cluster structures using the optical absorption spectroscopy.

V. CONCLUSION

In this work we have calculated the optical absorption spectra for several BN fullerenes in the size range of B_nN_n, $n=12–36$. Differences between the molecules and even between different isomers are observed in the near ultraviolet energy region. This consolidates the view that the TDDFT can be effectively used in determining and predicting the optical properties of middle-sized molecules and clusters. It has already been shown before that through the mutual interplay between calculations and experiments, the study of optical properties is a useful means of characterizing new materials. As the available computer resources expand and the TDDFT methods advance, contributions of the TDDFT in characterization, tailoring, or even designing new specific materials are expected to strongly increase.

[1] N. G. Chopra, R. J. Luyken, K. Cherrey, V. H. Crespi, M. L. Cohen, S. G. Louie, and A. Zettl, Science **269**, 966 (1995).
[2] L. Boulanger, B. Andriot, M. Cauchetier, and F. Willaime, Chem. Phys. Lett. **234**, 227 (1995).
[3] O. Stéphan, Y. Bando, A. Loiseau, F. Willamie, N. Shramchenko, T. Tamiya, and T. Sato, Appl. Phys. A: Mater. Sci. Process. **67**, 107 (1998).
[4] *A Primer in Density Functional Theory*, edited by C. Fiolhais, F. Nogueira, and M. Marques (Springer-Verlag, Berlin, 2003).
[5] G. Onida, L. Reining, and A. Rubio, Rev. Mod. Phys. **74**, 601 (2002).
[6] A. Castro, M. A. L. Marques, J. A. Alonso, and A. Rubio, J. Comput. Theor. Nanosci. **1**, 230 (2004).
[7] M. A. L. Marques and S. Botti, J. Chem. Phys. **123**, 014310 (2005).
[8] A. Castro, M. A. L. Marques, J. A. Alonso, G. F. Bertsch, K. Yabana, and A. Rubio, J. Chem. Phys. **116**, 1930 (2002).
[9] D. L. Strout, J. Phys. Chem. A **105**, 261 (2001).
[10] G. Seifert, P. W. Fowler, D. Mitchell, D. Porezag, and T. Frauenheim, Chem. Phys. Lett. **268**, 352 (1997).
[11] T. Oku, A. Nishiwaki, I. Narita, and M. Gonda, Chem. Phys. Lett. **380**, 620 (2003).
[12] T. Oku, A. Nishiwaki, and I. Narita, Sci. Technol. Adv. Mater. **5**, 635 (2004).
[13] T. Oku, A. Nishiwaki, and I. Narita, Physica B **351**, 184 (2004).
[14] H.-S. Wu and H. Jiao, Chem. Phys. Lett. **386**, 369 (2004).
[15] R. R. Zope, T. Baruah, M. R. Pederson, and B. I. Dunlap, Chem. Phys. Lett. **393**, 300 (2004).
[16] R. R. Zope, T. Baruah, M. R. Pederson, and B. I. Dunlap, Phys. Rev. A **71**, 025201 (2005).
[17] H.-S. Wu, X.-Y. Cui, and X.-H. Xu, J. Mol. Struct.: THEOCHEM **717**, 107 (2005).
[18] V. V. Pokropivny, V. V. Skorokhod, G. S. Oleinik, A. V. Kurdyumov, T. S. Bartnitskaya, A. V. Pokropivny, A. G. Sisonyuk, and D. M. Sheichenko, J. Solid State Chem. **154**, 214 (2000).
[19] T. Oku, A. Nishiwaki, and I. Narita, Solid State Commun. **130**, 171 (2004).
[20] V. Barone, A. Koller, and G. E. Scuseria, J. Phys. Chem. A **110**, 10844 (2006).
[21] J. M. Soler, E. Artacho, J. D. Gale, A. García, J. Junquera, P. Ordejón, and D. Sánchez-Portal, J. Phys.: Condens. Matter **14**, 2745 (2002); http://www.uam.es/departamentos/ciencias/fismateriac/siesta/
[22] A. Castro, H. Appel, M. Oliveira, C. A. Rozzi, X. Andrade, F. Lorenzen, M. A. L. Marques, E. K. U. Gross, and A. Rubio, Phys. Status Solidi B **243**, 2465 (2006); http://www.tddft.org/programs/octopus/
[23] *Time-Dependent Density Functional Theory*, edited by M. A. L. Marques, C. A. Ullrich, F. Nogueira, A. Rubio, K. Burke, and E. K. U. Gross (Springer-Verlag, Berlin, 2006).
[24] J. P. Perdew and A. Zunger, Phys. Rev. B **23**, 5048 (1981).
[25] J. P. Perdew, K. Burke, and M. Ernzerhof, Phys. Rev. Lett. **77**, 3865 (1996).
[26] N. Troullier and J. L. Martins, Phys. Rev. B **43**, 1993 (1991).
[27] M. A. L. Marques, A. Castro, and A. Rubio, J. Chem. Phys. **115**, 3006 (2001).